Journal of Radiation Research, Vol. 64, No. 2, 2023, pp. 317–327
https://doi.org/10.1093/jrr/rrac096
Advance Access Publication: 11 January 2023

Optimal timing of a γH2AX analysis to predict cellular lethal damage in cultured tumor cell lines after exposure to diagnostic and therapeutic radiation doses

Seiya Takano[1,*], Yuta Shibamoto[2], Zhen Wang[3], Takuhito Kondo[1,4], Shingo Hashimoto[5], Tatsuya Kawai[1] and Akio Hiwatashi[1]

[1]Department of Radiology, Nagoya City University Graduate School of Medical Sciences, Nagoya, 1 Kawasumi, Mizuho-cho, Mizuho-ku, Nagoya, Aichi, 467-8601, Japan
[2]Narita Memorial Proton Center, 78 Shirakawa-cho, Toyohashi, Aichi, 441-8021, Japan
[3] Gunma University Heavy Ion Medical Center, 3-39-22 Showa-machi, Maebashi, Gunma 371-8511, Japan
[4]Department of Radiology, Nagoya Ekisaikai Hospital, 4-66 Syonen-cyo, Nakagawa-ku, Nagoya, Aichi 454-8502, Japan
[5]Department of Radiation Oncology, Aichi Cancer Center Hospital, 1-1 Kanokoden, Chikusaku, Nagoya, Aichi 464-8681, Japan
*Corresponding author. Seiya Takano, MD, Department of Radiology, Nagoya City University Graduate School of Medical Sciences, 1 Kawasumi, Mizuhocho, Mizuho-ku, Nagoya, Aichi, 467-8601, Japan. Phone: (+81)52-853-8276; Fax: (+81)52-852-5244; E-mail: stakano6213@gmail.com
(Received 14 October 2022; revised 24 November 2022; editorial decision 28 November 2022)

ABSTRACT

Phosphorylated H2AX (γH2AX) is a sensitive biomarker of DNA double-strand breaks (DSBs). To assess the adverse effects of low-dose radiation (<50 mGy), γH2AX levels have typically been measured in human lymphocytes within 30 min of computed tomography (CT) examinations. However, in the presence of DSB repair, it remains unclear whether γH2AX levels within 30 min of irradiation completely reflect biological effects. Therefore, we investigated the optimal timing of a γH2AX analysis to predict the cell-surviving fraction (SF). Three tumor cell lines were irradiated at different X-ray doses (10–4000 mGy), and the relationships between SF and relative γH2AX levels were investigated 15 min and 2, 6, 12 and 24 h after irradiation. Data were analyzed for high-dose (0–4000 mGy) and low-dose (0–500 mGy) ranges. Correlations were observed between SF and the relative number of γH2AX foci/nucleus at 12 h only ($R^2 = 0.68$, $P = 0.001$ after high doses; $R^2 = 0.37$, $P = 0.016$ after low doses). The relative intensity of γH2AX correlated with SF 15 min to 12 h after high doses and 2 to 12 h after low doses, with the maximum R^2 values being observed 2 h after high doses ($R^2 = 0.89$, $P < 0.001$) and 12 h after low doses ($R^2 = 0.65$, $P < 0.001$). Collectively, cellular lethal damage in tumor cells was more accurately estimated with residual DSBs 12 h after low-dose (10–500 mGy) irradiation. These results may contribute to determination of the optimal timing of biodosimetric analyses using γH2AX in future studies.

Keywords: gammaH2AX (γH2AX); double-strand break (DSB); clonogenic cell survival; DNA repair; low-dose radiation

INTRODUCTION

The risk of cancer has been suggested to increase following diagnostic X-ray examinations [1–3], and concerns have been expressed regarding the negative impact of low-dose radiation in computed tomography (CT) examinations on the incidence of cancer. Although the results need to be interpreted cautiously [4, 5], it seems important to assess the adverse effects of diagnostic X-ray examinations, and DNA double-strand breaks (DSBs) have been measured in the lymphocytes of individuals undergoing CT or angiographic examinations. DSBs are the most lethal lesions produced by ionizing radiation, and if not adequately repaired, may lead to cell death, genome instability and carcinogenesis [6]. Recent studies reported increases in DSBs even after exposure to a diagnostic level of radiation (<50 mGy) in CT and coronary angiography (CAG) based on the scoring of phosphorylated histone H2AX (γH2AX) foci in human peripheral blood lymphocytes within 30 min of these examinations [7–9]. However, it is unclear

whether a γH2AX analysis within 30 min of irradiation completely reflects biological effects because the majority of radiation-induced DSBs are repaired over a period of hours [10, 11].

The immunofluorescence staining of γH2AX is widely used to score DSBs induced by radiation at as low as 6 mGy [12–14]. The phosphorylation of H2AX proteins occurs as an early step in DSBs and the yield of γH2AX foci peaks within 30 min of irradiation [15]. Thereafter, γH2AX foci decrease with DNA repair [16, 17]. In normal human fibroblasts and tumor cells, residual γH2AX foci 12–24 h after irradiation have been shown to reflect the DSBs that are more difficult to be repaired, and correlate more closely with the cell-surviving fraction (SF) or radiosensitivity than initial γH2AX foci [18–22]. Therefore, we assumed that cell viability or lethal damage may be more accurately estimated with residual γH2AX foci observed at least a few hours after irradiation. However, limited information is currently available on how and to what extent the relationship between DSBs and cellular lethal damage varies during a period of hours after irradiation. Furthermore, since the majority of studies focused on radiation doses relevant to radiotherapy (≥1 Gy), the effects of lower doses remain unknown. Therefore, we herein performed an *in vitro* time-course study of low (0–500 mGy) and high (0–4000 mGy) dose ranges in cultured human and mammalian tumor cell lines. The aim of the present study was to elucidate the optimal timing of a γH2AX analysis in order to predict SF. Cell SF was used as a common endpoint to represent cellular damage. Since SF determined by colony assay was an endpoint to be compared with γH2AX indices, normal cells could not be used in this study.

MATERIALS AND METHODS

Cell lines and culture conditions

The mouse melanoma cell line B16F0, mouse mammary tumor cell line EMT6, and human cervical tumor cell line HeLa S3 were used. B16F0 cells were purchased from the American Type Culture Collection (Virginia, USA). EMT6 cells were a gift from Stanford University (Prof. R. F. Kallman) and were obtained through Kyoto University [23]. HeLa S3 cells were purchased from the Riken Cell Bank (Tokyo, Japan). All cell lines were negative for mycoplasma infection. Cells were incubated in a humidified atmosphere of 95% air/5% CO_2 at 37°C and serially passaged every week. EMT6 cells were cultured with Eagle's minimum essential medium (Nissui Pharmaceutical Co., Ltd., Tokyo, Japan) and B16F0 and HeLa cells with Dulbecco's modified Eagle medium (Wako Pure Chemical Industries, Ltd., Osaka, Japan), both of which were supplemented with 13% fetal bovine serum and antibiotics (100 U/mL penicillin–streptomycin).

Colony formation assay

Exponentially growing cells were divided into seven groups and seeded on 10-cm plastic dishes. After a 24-h incubation, cells were irradiated at 0, 10, 50, 150, 500, 2000 and 4000 mGy with an X-ray apparatus (CAX-210; Chubu Medical Co., Ltd., Yokkaichi, Japan; 210 kV, 10 mA, 4-mm Al and 2-mm Cu filters). The dose rate was 495 mGy/min. Fixation with 80% ethanol and staining with 5% Giemsa reagent were performed 7 days after irradiation for B16F0 and EMT6 cells and 10 days after irradiation for HeLa cells. Colonies containing 50 or more cells were counted. Cell survival was assessed based on the plating efficiency of irradiated cells divided by that of non-irradiated cells. Three independent experiments were performed per cell line. Plots of clonogenic survival were fit according to the linear quadratic model: $SF = \exp(-\alpha D - \beta D^2)$, where D is the dose in Gy, and α (Gy^{-1}) and β (Gy^{-2}) are the fitting parameters. As an indicator of radiation sensitivity, SF after 2 Gy (SF2) was also calculated.

Immunofluorescence staining of phosphorylated H2AX

To evaluate the kinetics of DNA DSBs, the immunofluorescence staining of γH2AX was performed at various doses and post-irradiation time points. Our method of immunofluorescence staining was previously described [24, 25]. Briefly, the three cell lines (B16F0, EMT6 and HeLa S3) were seeded on 96-well plates, and after a 24-h incubation, were exposed to 0-, 10-, 50-, 150-, 500-, 2000- and 4000-mGy doses at the same dose rate as in the colony formation assay. Cells were allowed to repair DSBs at 37°C. Fifteen minutes and 2, 6, 12 and 24 h after irradiation, cells were fixed with 3.7% formaldehyde, permeabilized in 90% methanol, and incubated in blocking/antibody incubation buffer (1% bovine serum albumin/PBS) for 30 minutes. Nuclei were stained with 4', 6-diamidino-2-phenylindole (DAPI; Thermo Scientific, Waltham, MA). γH2AX foci were detected with the primary antibody, anti-phospho-histone H2AX (×100, Ser 139, OxiSelect DNA SDB Staining Kit; Cell Biolabs, Inc., San Diego, CA) and then with the secondary antibody, fluorescein isothiocyanate-conjugated goat antimouse IgG (×100, OxiSelect DNA DSB Staining Kit). The number and fluorescence intensity of γH2AX foci in at least 200 cells per group were scored by automated fluorescence microscopy (IN Cell Analyzer 6000; GE Healthcare UK Ltd, UK).

The number and fluorescence intensity of γH2AX foci may be affected by cell proliferation at later time points [18, 26, 27]. Therefore, the total numbers of cell nuclei stained with DAPI were scored with 72-field automated fluorescence microscopy in each dose group at each post-irradiation time point. To estimate the duration of the cell cycle, doubling times of the three cell lines were calculated in each non-irradiated group under the assumption that one nucleus represents one cell.

Statistical analysis

Differences in the number or fluorescence intensity of γH2AX among the dose groups (0, 10, 50, 150, 500, 2000 and 4000 mGy) were analyzed using a one-way analysis of variance (ANOVA) followed by Dunnett's test for a post hoc analysis. A linear regression analysis was performed to evaluate the linear relationship between log-transformed SF and γH2AX levels at each time point. A sampling time point with the significantly highest coefficient of determination (R^2) value was considered to be the optimal time point to predict SF. R^2 values were obtained from a linear regression analysis. The number of γH2AX foci/nucleus and the fluorescence intensity of γH2AX were both expressed as relative values to the control group. Differences in the numbers of cell nuclei among the dose groups were analyzed using a one-way ANOVA followed by Dunnett's test for a post hoc analysis. All data were represented as the mean ± standard deviation (SD). All statistical analyses were conducted using R Version 3.6.3 (The R

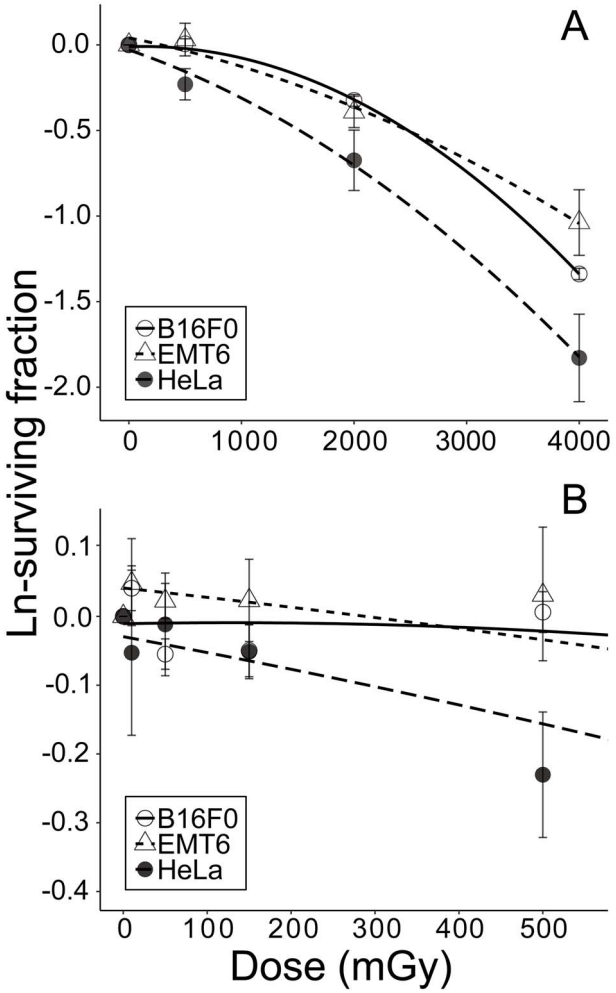

Fig. 1. Dose-survival curves of B16F0, EMT6 and HeLa S3 cells. Data represent means and SDs from three separate experiments.

Foundation for Statistical Computing, Vienna, Austria). The threshold for significance was $P < 0.05$.

RESULTS

Dose-survival curves of tumor cells

Figure 1 shows dose-survival curves for B16F0, EMT6 and HeLa S3 cells after X-ray irradiation. The three tumor cell lines showed high plating efficiencies (mean, 0.77–0.99) with no significant differences. In dose-survival curves, EMT6 and B16F0 cells showed slightly higher SF than HeLa cells at doses ≥500 mGy (Fig. 1). At doses ≤150 mGy, no significant differences were observed in the mean values of SF among the cell lines (data not shown). The SF2 values of B16F0, EMT6 and HeLa cells were 0.72 ± 0.025, 0.68 ± 0.061 and 0.51 ± 0.085 (mean ± SD), respectively (Table 1). The mean SF2 value of B16F0 was significantly higher than that of HeLa (ANOVA, $P = 0.032$).

Characteristics of three cell lines

The characteristics of cellular growth and endogenous γH2AX foci expression (background level) are shown in Table 1. B16F0 and EMT6 cells showed shorter doubling times than HeLa cells ($P = 0.0093$ and 0.0068, respectively). The background γH2AX fluorescence intensity of B16F0 cells was significantly higher than that of HeLa cells ($P = 0.024$). Regarding other parameters, including background γH2AX foci/nucleus and the proportion of cells with endogenous γH2AX foci, no significant differences were noted among the three cell lines. The proportions of cells with endogenous γH2AX foci were 0.89 ± 0.064 in B16F0 cells, 0.66 ± 0.29 in EMT6 cells and 0.61 ± 0.11 in HeLa cells (mean ± SD).

Changes in phosphorylated H2AX levels after X-ray irradiation

Figure 2 shows changes in γH2AX levels after exposure to various doses of X-rays (0, 10, 50, 150, 500, 2000 and 4000 mGy). Representative photomicrographic images of DAPI and γH2AX immunofluorescence staining at different time points are shown in Fig. 3. The mean number of γH2AX foci/nucleus increased by four- to six-fold after 15 min in all cell lines; significant increases were observed at doses ≥2000 mGy in EMT6 cells and ≥ 500 mGy in B16F0 and HeLa cells. After doses ≥2000 mGy, the mean number of γH2AX foci remained significantly higher than those of the respective control groups up to 6 h later. However, by 12 h after irradiation, γH2AX foci decreased to negligible levels in B16F0 and EMT6 cells. In contrast, 56% of γH2AX foci generated at 15 min were still present 12 h after irradiation with 4000 mGy in HeLa cells. No significant differences were observed among different dose groups or cell lines after 24 h.

Similar results were observed for the relative fluorescence intensity of γH2AX, although some differences were found. The mean relative fluorescence intensity for all cell lines increased by two- to three-fold after 15 min. Significantly higher fluorescence levels were observed 15 min after irradiation with 150 mGy in HeLa cells, and up to 83 and 54% of fluorescence levels after 15 min remained even 12 h after 4000 mGy in B16F0 and HeLa cells, respectively. Similar to the results obtained on the kinetics of γH2AX foci, no significant differences were observed among different doses after 24 h.

Relationships between the cell-surviving fraction and phosphorylated H2AX levels

The relationships between SF and relative γH2AX levels at each specific time point, stratified into high- (0, 500, 2000 and 4000 mGy) and low-dose (0, 10, 50, 150 and 500 mGy) ranges, are shown in Figs 4 and 5. Data were shown separately based on the two different measurement methods, i.e. the relative number of γH2AX foci/nucleus (Fig. 4) and the relative intensity of γH2AX (Fig. 5). Regarding the relative number of γH2AX foci/nucleus, R^2 values 12 h after both high-dose ($R^2 = 0.68$, $P = 0.001$) and low-dose irradiation ($R^2 = 0.37$, $P = 0.016$) were higher than those at the other time points (Fig. 4). At all time points, except for 12 h, foci numbers did not correlate with SF. Regarding the relative intensity of γH2AX, correlations were observed from 15 min to 12 h for the high-dose range and from 2 to 12 h for the

Table 1. Characteristics of three cell lines

Cell line	Plating efficiency	SF2	α (Gy^{-1})	β (Gy^{-2})	Doubling time (h)	Background γH2AX foci/nucleus	Background γH2AX fluorescence intensity	Proportion of cells with endogenous γH2AX foci (%)
B16F0	0.89 ± 0.026	0.72 ± 0.025[a]	-0.023	0.089	11 ± 1.2[b]	14 ± 2.1	$13\,100 \pm 537$[d]	89 ± 6.4
EMT6	0.99 ± 0.057	0.68 ± 0.061	0.13	0.035	11 ± 1.5[c]	7.2 ± 6.9	$10\,600 \pm 5040$	66 ± 29
HeLa S3	0.77 ± 0.11	0.51 ± 0.085[a]	0.23	0.056	16 ± 0.43[b,c]	6.9 ± 3.1	2300 ± 470[d]	61 ± 11

SF2 = surviving fraction at 2 Gy.
[a] $P = 0.032$ [b] $P = 0.0093$ [c] $P = 0.0068$, and [d] $P = 0.024$ by a one-way analysis of variance followed by Tukey's test for a post hoc analysis. Data represent the mean ± SD of three independent experiments.

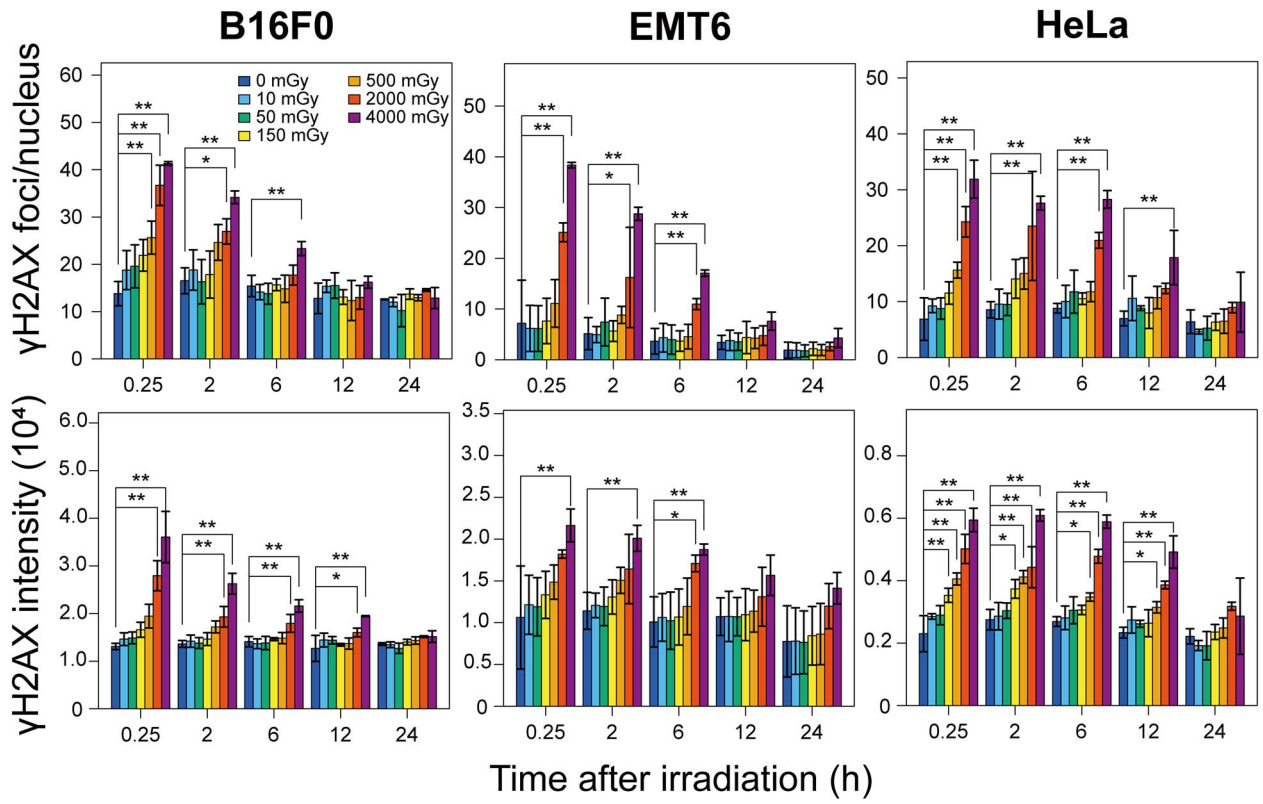

Fig. 2. Changes in γH2AX levels after exposure to various doses of X-rays (0, 10, 50, 150, 500, 2000 and 4000 mGy) in B16F0, EMT6 and HeLa S3 cells. Data represent means and standard errors from three separate experiments. * $P < 0.05$, ** $P < 0.01$.

low-dose range. As a result, R^2 values 2 h after high doses ($R^2 = 0.89$, $P < 0.001$) and 12 h after low doses ($R^2 = 0.65$, $P < 0.001$) were the highest (Fig. 5).

Further analyses of the plots at 12 h with a linear regression yielded the following equations: Ln SF = -0.89 x + 0.80 for γH2AX foci at high doses; Ln SF = -0.23 x + 0.24 for γH2AX foci at low doses; Ln SF = -1.69 x + 1.75 for γH2AX intensity at high doses; Ln SF = -0.55 x + 0.59 for γH2AX intensity at low doses, where x is the relative level of γH2AX to the control. Regression coefficients at high doses were generally two- to three-fold smaller than at low doses.

Analyses of cell proliferation

The numbers of cell nuclei stained with DAPI observed under 72 fields of automated fluorescence microscopy are shown in Fig. 6. The doubling times of B16F0, EMT6 and HeLa cells were 11 ± 1.2 h, 11 ± 1.5 h and 16 ± 0.43 h (mean ± SD), respectively (Table 1). Figure 7 is representative photomicrographic images showing the proliferation of EMT6 cells 24 h after irradiation. The number of cell nuclei was significantly lower in EMT6 and HeLa cells than in the control 12 and 24 h after irradiation with 4000 mGy. The results obtained for B16F0 were similar; however, no significant differences were observed.

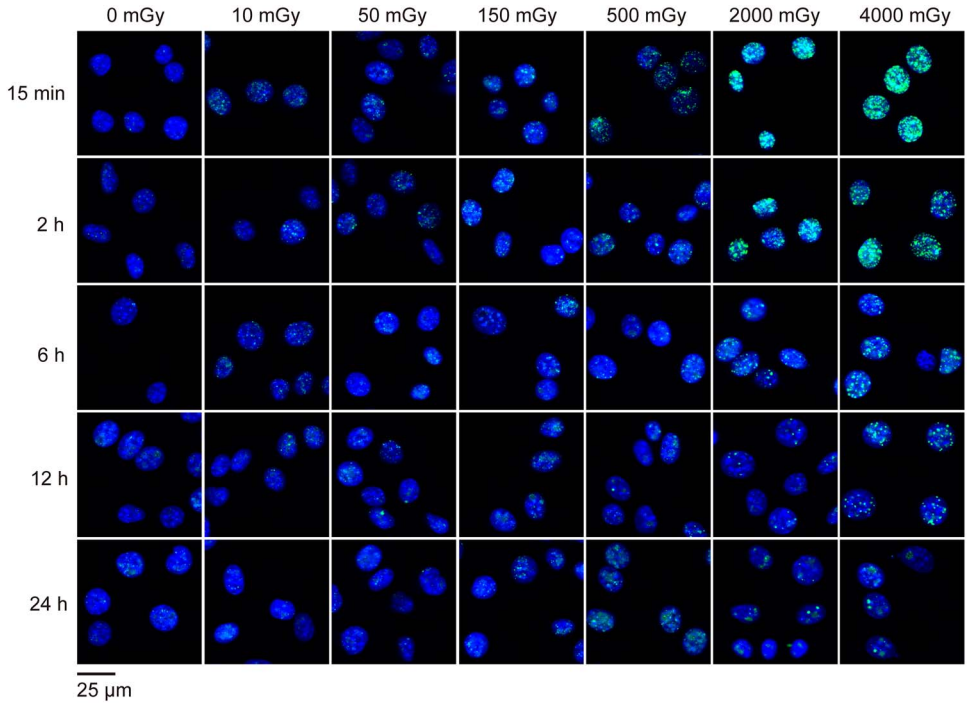

Fig. 3. Representative images of 4',6-diamidino-2-phenylindole (DAPI) and phosphorylated histone H2AX (γH2AX) staining in mouse melanoma (B16F0) cells 15 min and 2, 6, 12 and 24 h after exposure to X-ray doses of 0, 10, 50, 150, 500, 2000 and 4000 mGy. Green, γH2AX; blue, DAPI. The bar corresponds to 25 μm.

DISCUSSION

The carcinogenic risks associated with exposure to low-dose radiation in CT scans and other diagnostic imaging examinations remain controversial [28, 29]. Previous studies that investigated the incidence of cancer in cohorts undergoing CT during childhood showed a higher incidence of leukemia, brain tumors and other malignancies [1, 3, 4]. However, in a recent study, a large bias was found in the background between children undergoing CT and those not undergoing CT [5]; more than one-third of children undergoing CT scans had a congenital anomaly and those with an anomaly had an approximately 3-fold higher risk of developing cancer. Therefore, it is considered inappropriate to conclude that CT scans during childhood are associated with an increased risk of developing cancer. An experimental study suggested that CT scans on cancer-prone mice increased survival times and the latency period before the development of sarcoma and lymphoma [30, 31]. Recent studies indicated that continuous low-dose irradiation produced radioadaptive responses in cultured cells [24], decreases in γH2AX indices 24 h after irradiation with 2 Gy [24], the growth promotion of silkworm larvae [32, 33], and delays in tumor development after the transplantation of tumor cells in syngeneic mice [33]. Therefore, more attention is being paid to the potentially beneficial effects of low-dose radiation. In the present study, no increases in γH2AX indices were observed ≥15 min after irradiation with ≤150 mGy in all three cell lines.

In previous studies showing increases in γH2AX indices in human lymphocytes after CT scans and CAG [7–9], initial γH2AX foci within 30 min of irradiation were regarded as an indicator of DNA damage, and increases were suggested to be associated with cancer risks. In other studies, the number of initial γH2AX foci after CT scans showed a linear dose response [14, 34] or low-dose hypersensitivity [9]. However, initial γH2AX foci only represent the number of DSBs generated, which may be helpful for estimating the actual irradiated dose, but may not be appropriate to assess overall biological effects, including the risks of tissue damage and cancer development [12]. Instead, the kinetics of DSB repair need to be considered since the majority of initial DSBs are repaired within a few hours of irradiation [10, 11]. Therefore, a γH2AX analysis may be more reasonable if performed at least a few hours of irradiation, and we herein investigated the relationship between DSBs and SF to select the optimal timing of a γH2AX analysis. We assumed that the optimal timing to estimate cellular lethal damage from a γH2AX analysis will be helpful for selecting the optimal timing to estimate genetic damage leading to carcinogenesis.

Consistent with previous findings [15], the mean levels of γH2AX foci/nucleus and γH2AX intensity were the highest 15 min after irradiation and decreased thereafter (Fig. 2). A clear dose response was apparent 15 min after irradiation. γH2AX foci are dephosphorylated with DSB repair [16]. DSB repair has two components: non-homologous end-joining (NHEJ) and homologous recombination. Approximately 80% of radiation-induced DSBs are rejoined by NHEJ [35], and, thus, most DSBs are assumed to be associated with a risk of genomic rearrangements based on the error-prone nature of NHEJ. However, it currently remains unclear whether NHEJ following low-dose irradiation causes genomic rearrangements, and a previous study showed a low incidence of genomic rearrangements by NHEJ in

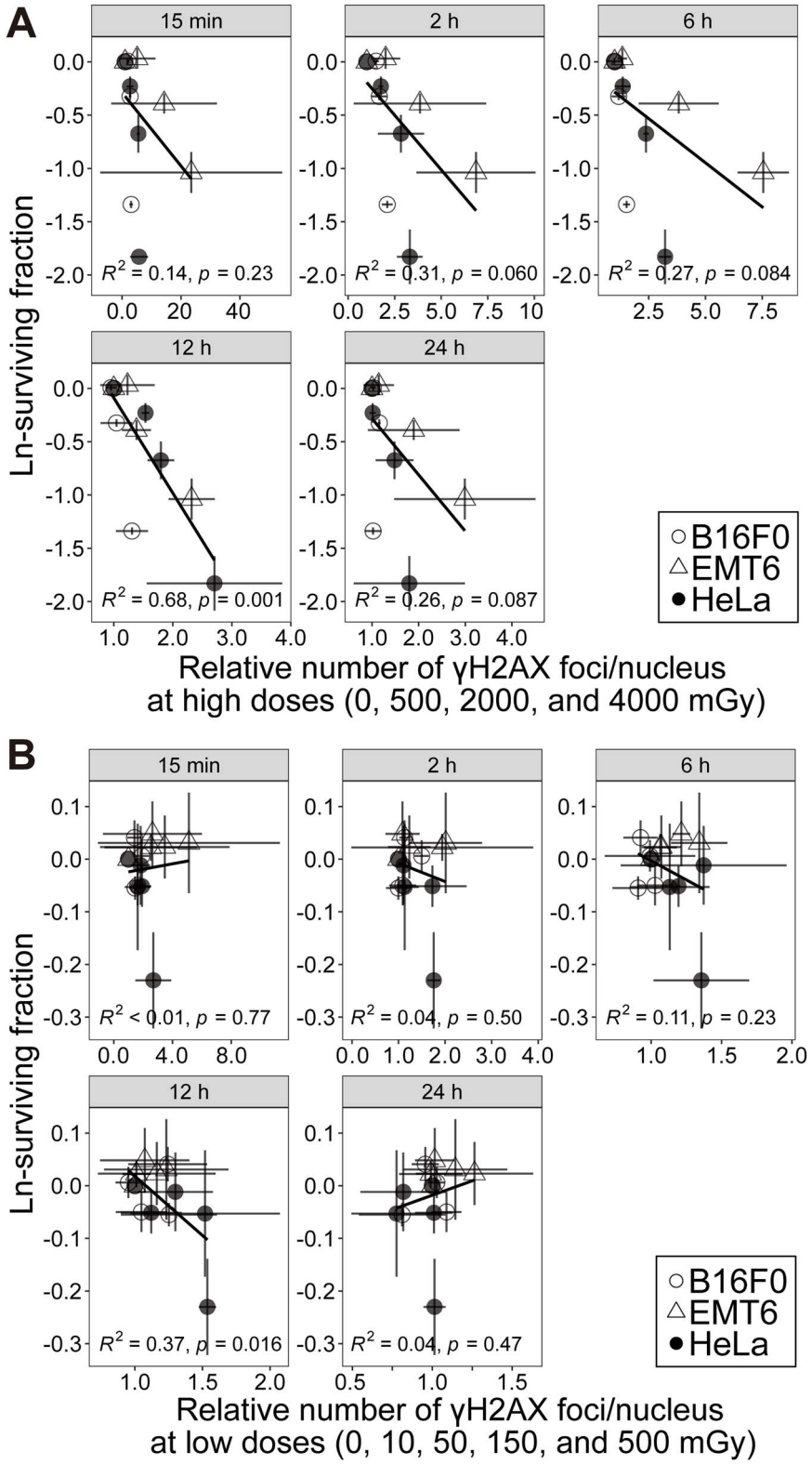

Fig. 4. Relationships between SF and the relative number of phosphorylated histone H2AX (γH2AX) foci/nucleus in B16F0, EMT6 and HeLa S3 cells in (A) high-dose and (B) low-dose ranges. Data represent means and SDs from three separate experiments.

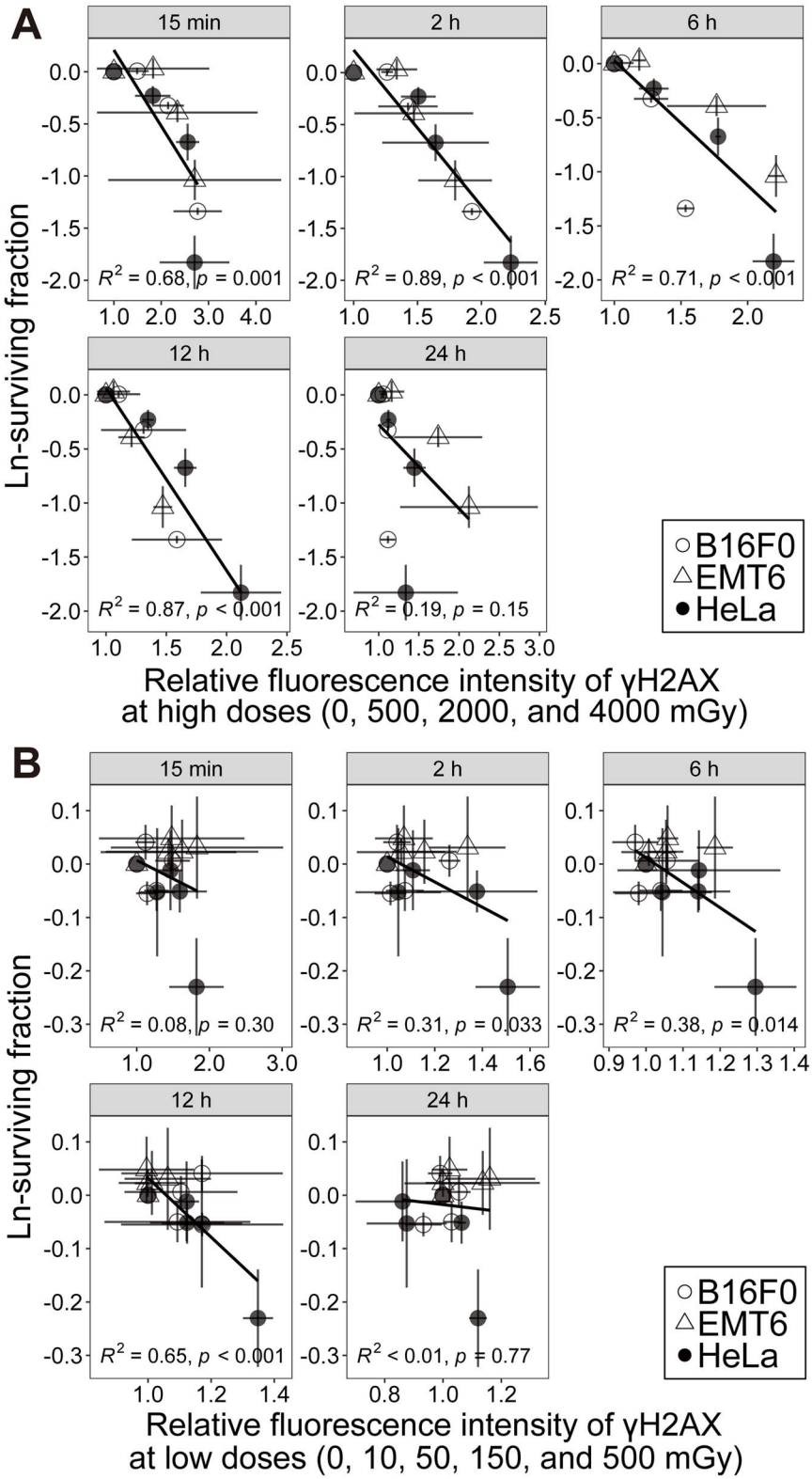

Fig. 5. Relationships between SF and the relative fluorescence intensity of phosphorylated histone H2AX (γH2AX) in B16F0, EMT6 and HeLa S3 cells in (A) high-dose and (B) low-dose ranges. Data represent means and SDs from three separate experiments.

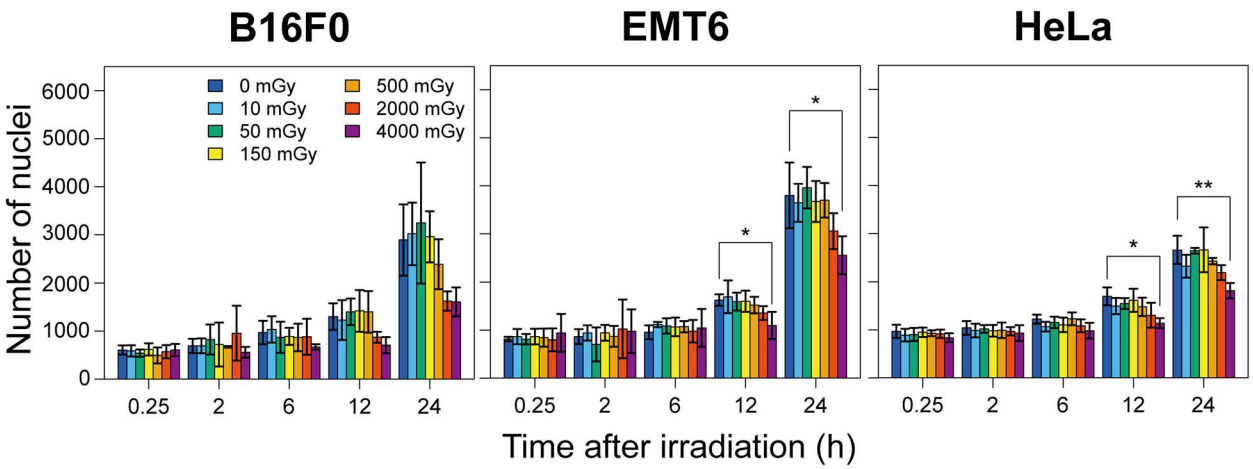

Fig. 6. Total numbers of cell nuclei 15 min and 2, 6, 12 and 24 h after exposure to X-ray doses of 0, 10, 50, 150, 500, 2000 and 4000 mGy for analysis of cell proliferation in B16F0, EMT6 and HeLa S3 cells. Cell nuclei stained with 4', 6-diamidino-2-phenylindole (DAPI) were scored with 72-field automated fluorescence microscopy. Data represent means and standard errors from three separate experiments. * $P < 0.05$, ** $P < 0.01$.

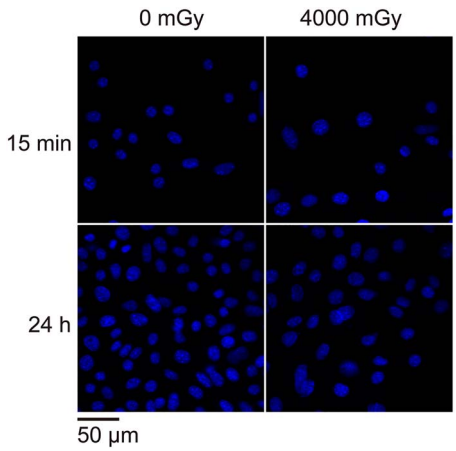

Fig. 7. Representative images showing cell proliferation of mouse mammary tumor (EMT6) cells 15 min and 24 h after exposure to X-ray doses of 0 and 4000 mGy. Cell nuclei stained with 4', 6-diamidino-2-phenylindole (DAPI) were scored with 72-field automated fluorescence microscopy. Blue, DAPI. The bar corresponds to 50 μm.

normal mammalian cell lines [36]. The rate of decreases in γH2AX levels appeared to differ among the three cell lines examined (Fig. 2). HeLa cells showed the slower disappearance of γH2AX foci than B16F0 and EMT6 cells. This may have resulted in the higher radiation sensitivity of HeLa cells, as indicated by lower SF2 (Table 1). This was consistent with previous findings showing a correlation between the half-life of the loss of γH2AX foci and radiation sensitivity in tumor cells [37, 38]. ATM and p53 defects may influence cellular radiation sensitivity [19]; however, gene expression statuses were not investigated in the present study. Furthermore, the slow proliferation rates of HeLa cells may also be related, as discussed later.

In contrast to previous findings [19–22], no significant differences were observed in γH2AX levels among different doses 24 h after irradiation, although slight dose responses were detected (Fig. 2). This result may be explained as follows. The endogenous expression of γH2AX (background level) may affect the ability to detect small amounts of residual DSBs [39]. The tumor cell lines used in the present study showed high proportions of endogenous γH2AX expression (61–89%), as shown in Table 1. In normally proliferating cells, the formation of γH2AX foci may also occur in M-phase chromosomes [40] and at stalled replication forks in S-phase cells [27] even without exogenous DNA damage. Under these conditions, non-replicating G0/G1 cells may be suitable for a more accurate γH2AX analysis. Furthermore, we need to consider the effects of cell proliferation. Cell proliferation was most prominent 24 h after irradiation in the three cell lines although the proliferation rate tended to decrease as the irradiated dose increased (Fig. 6). However, even at doses $\geq$2000 mGy, the number of tumor cells increased by two- to three-fold in 24 hours (Fig. 6). In addition, relative γH2AX foci/nucleus and relative γH2AX intensity were mean values per number or area of nuclei. These units are essentially affected by the number of the population. Therefore, we may have underestimated the mean γH2AX value 24 h after irradiation, for example, due to the predominant proliferation of intact cells that had completed DSB repair and restarted the cell cycle. In proliferating cells, the correlation between clonogenic survival and γH2AX foci may disappear at the time point beyond the duration of the cell cycle due to the disassembly of γH2AX foci during mitosis [18]. Considering the cell cycle times (11 h for B16F0 and EMT6 and 16 h for HeLa, Table 1) and cell proliferation data (Fig. 6), up to 12 h after irradiation seemed to be acceptable for a γH2AX analysis in the present study, although the distribution of the cell cycle may also have affected the accuracy of measurement after high doses [26, 27].

We also examined the optimal timing to predict SF (Figs 4 and 5). Previous studies showed that residual γH2AX foci 12–24 h after irradiation correlated with SF in normal human fibroblasts and tumor

cells [18–22]; however, they mainly used doses employed in radiotherapy (≥1 Gy). We found that γH2AX levels after 12 h were most consistently associated with SF in a low-dose range (≤500 mGy), while no correlations were observed 15 min after irradiation. Therefore, the present results suggest that DSBs remaining 12 h after low-dose (≤500 mGy) irradiation may be more likely to cause clonogenic cell death than initial DSBs, although the results in the low-dose range must be carefully interpretated because of the large inter-experimental variations (Figs 4B and 5B). In the high-dose range, the results were partly inconsistent between relative γH2AX foci/nucleus and relative γH2AX intensity (Figs 4A and 5A). According to previous studies, overlapping of γH2AX foci, as also seen in the present study (Fig. 3), may lead to distorted dose–response at high doses (≥ 2 Gy) with automatic counting of γH2AX foci, while γH2AX intensity provides more reliable results up to 5 Gy [41, 42]. Accordingly, based on the results of γH2AX intensity (Fig. 5A), we assumed that the optimal timing may be from 15 min to 12 h after high-dose (500–4000 mGy) irradiation. There are several findings in the literature showing a correlation between initial DSBs and cellular radiosensitivity in various human cancer cells, including HeLa cells [43, 44]. If 10–20 DSBs occur after high doses (≥2 Gy) of irradiation, the G2/M checkpoint may be unable to sufficiently function [45]. Under these conditions, cells go into mitosis with a large amount of residual DSBs, which may lead to chromosomal breaks and cell death. These findings imply that the extent of DSB repair has less of an impact on SF after high doses (≥2 Gy) unless the number of DSBs is reduced below a certain threshold. Further studies are warranted to confirm this disparity between low and high doses.

The present study has some limitations. We did not investigate other proteins related to DSB repair besides γH2AX. γH2AX foci do not always represent the residual DSBs because γH2AX may co-localize with the sites of DSBs even after NHEJ has been completed [46]. Furthermore, the present results cannot be directly applied to the incidence of genomic rearrangements, which play an important role in carcinogenesis. In addition, we selected tumor cell lines due to the ease of calculating SF in proliferating cells. Therefore, our results may not necessarily apply to peripheral blood lymphocytes or normal human cells, although there appear no data suggesting quite different patterns in DSB repair between normal cells and tumor cells [18, 39, 47]. Ideally, similar experiments should also be performed in peripheral blood lymphocytes and normal human cells to assess the adverse effects of CT examinations. In that case, another endpoint other than clonogenicity may be needed to estimate cellular lethal damage since normal cells have low plating efficiency.

In conclusion, we herein demonstrated that cellular lethal damage in tumor cells was more accurately estimated with residual DSBs 12 h after low-dose (10–500 mGy) irradiation. Therefore, a delayed γH2AX analysis may need to be considered in future biodosimetric studies which we are planning to investigate the effects of low-dose radiation in diagnostic imaging, such as CT scans. Further studies are warranted to determine the optimal timing of a γH2AX analysis in peripheral blood lymphocytes and normal human cells.

ACKNOWLEDGEMENTS

The present study was performed in part at the Core Laboratory, Nagoya City University Graduate School of Medical Sciences. The authors are grateful to Mr. Hiroshi Takase for his technical support.

FUNDING

This work was supported in part by JSPS KAKENHI (18K07725, 19K17175).

CONFLICT OF INTEREST

The authors declare no potential conflicts of interest with respect to the research, authorship, or publication of this article.

REFERENCES

1. Pearce MS, Salotti JA, Little MP *et al.* Radiation exposure from CT scans in childhood and subsequent risk of leukaemia and brain tumours: a retrospective cohort study. *Lancet* 2012;380:499–505.
2. Brenner DJ. Radiation risks potentially associated with low-dose CT screening of adult smokers for lung cancer. *Radiology* 2004;231:440–5.
3. Mathews JD, Forsythe AV, Brady Z *et al.* Cancer risk in 680,000 people exposed to computed tomography scans in childhood or adolescence: data linkage study of 11 million Australians. *BMJ* 2013;346:f2360. https://doi.org/10.1136/bmj.f2360.
4. Huang R, Liu X, He L *et al.* Radiation exposure associated with computed tomography in childhood and the subsequent risk of cancer: a meta-analysis of cohort studies. *Dose Response* 2020;18. https://doi.org/10.1177/1559325820923828.
5. Shibata S, Shibamoto Y, Maehara M *et al.* Reasons for undergoing CT during childhood: can CT-exposed and CT-naive populations be compared? *Dose Response* 2020;18. https://doi.org/10.1177/1559325820907011.
6. Willers H, Dahm-Daphi J, Powell SN. Repair of radiation damage to DNA. *Br J Cancer* 2004;90:1297–301.
7. Sakane H, Ishida M, Shi L *et al.* Biological effects of low-dose chest CT on chromosomal DNA. *Radiology* 2020;295:439–45.
8. Alipoor A, Fardid R, Sharifzadeh S. Evaluating gamma-H2AX expression as a biomarker of DNA damage after X-ray in angiography patients. *J Biomed Phys Eng* 2018;8:393–402.
9. Vandevoorde C, Franck C, Bacher K *et al.* γ-H2AX foci as in vivo effect biomarker in children emphasize the importance to minimize x-ray doses in paediatric CT imaging. *Eur Radiol* 2015;25:800–11.
10. Chowdhury D, Keogh MC, Ishii H *et al.* γ-H2AX dephosphorylation by protein phosphatase 2A facilitates DNA double-strand break repair. *Mol Cell* 2005;20:801–9.
11. Jakl L, Marková E, Koláriková L *et al.* Biodosimetry of low dose ionizing radiation using DNA repair foci in human lymphocytes. *Genes (Basel)* 2020;11. https://doi.org/10.3390/genes11010058.
12. Rogakou EP, Boon C, Redon C *et al.* Megabase chromatin domains involved in DNA double-strand breaks in vivo. *J Cell Biol* 1999;146:905–15.
13. Roch-Lefévre S, Mandina T, Voisin P *et al.* Quantification of γ-H2AX foci in human lymphocytes: a method for

biological dosimetry after ionizing radiation exposure. *Radiat Res* 2010;174:185–94.
14. Rothkamm K, Balroop S, Shekhdar J *et al.* Leukocyte DNA damage after multi-detector row CT: a quantitative biomarker of low-level radiation exposure. *Radiology* 2007;242:244–51.
15. Rogakou EP, Pilch DR, Orr AH *et al.* DNA double-stranded breaks induce histone H2AX phosphorylation on serine 139. *J Biol Chem* 1998;273:5858–68.
16. Riballo E, Kühne M, Rief N *et al.* A pathway of double-strand break rejoining dependent upon ATM, Artemis, and proteins locating to γ-H2AX foci. *Mol Cell* 2004;16:715–24.
17. Keogh MC, Kim JA, Downey M *et al.* A phosphatase complex that dephosphorylates γH2AX regulates DNA damage checkpoint recovery. *Nature* 2006;439:497–501.
18. Marková E, Schultz N, Belyaev IY. Kinetics and dose-response of residual 53BP1/γ-H2AX foci: co-localization, relationship with DSB repair and clonogenic survival. *Int J Radiat Biol* 2007;83:319–29.
19. Mirzayans R, Severin D, Murray D. Relationship between DNA double-strand break rejoining and cell survival after exposure to ionizing radiation in human fibroblast strains with differing ATM/p53 status: implications for evaluation of clinical radiosensitivity. *Int J Radiat Oncol Biol Phys* 2006;66:1498–505.
20. Banáth JP, Klokov D, MacPhail SH *et al.* Residual γH2AX foci as an indication of lethal DNA lesions. *BMC Cancer* 2010;10. https://doi.org/10.1186/1471-2407-10-4.
21. Menegakis A, Yaromina A, Eicheler W *et al.* Prediction of clonogenic cell survival curves based on the number of residual DNA double strand breaks measured by gammaH2AX staining. *Int J Radiat Biol* 2009;85:1032–41.
22. Dikomey E, Brammer I, Johansen J *et al.* Relationship between DNA double-strand breaks, cell killing, and fibrosis studied in confluent skin fibroblasts derived from breast cancer patients. *Int J Radiat Oncol Biol Phys* 2000;46:481–90.
23. Shibamoto Y, Ito M, Sugie C *et al.* Recovery from sublethal damage during intermittent exposures in cultured tumor cells: implications for dose modification in radiosurgery and IMRT. *Int J Radiat Oncol Biol Phys* 2004;59:1484–90.
24. Wang Z, Sugie C, Nakashima M *et al.* Changes in the proliferation rate, clonogenicity, and radiosensitivity of cultured cells during and after continuous low-dose-rate irradiation. *Dose Response* 2019;17. https://doi.org/10.1177/1559325819842733.
25. Kondo T, Shibamoto Y, Kawai T *et al.* Effects of a combined treatment regimen consisting of Hsp90 inhibitor DS-2248 and radiation in vitro and in a tumor mouse model. *Transl Cancer Res* 2021;10:2767–76.
26. El-Awady RA, Dikomey E, Dahm-Daphi J. Radiosensitivity of human tumour cells is correlated with the induction but not with the repair of DNA double-strand breaks. *Br J Cancer* 2003;89:593–601.
27. Löbrich M, Shibata A, Beucher A *et al.* γH2AX foci analysis for monitoring DNA double-strand break repair: strengths, limitations and optimization. *Cell Cycle* 2010;9:662–9.
28. Shibamoto Y, Nakamura H. Overview of biological, epidemiological, and clinical evidence of radiation hormesis. *Int J Mol Sci* 2018;19. https://doi.org/10.3390/ijms19082387.
29. Oakley PA, Harrison DE. Death of the ALARA radiation protection principle as used in the medical sector. *Dose Response* 2020;18. https://doi.org/10.1177/1559325820921641.
30. Lemon JA, Phan N, Boreham DR. Single CT scan prolongs survival by extending cancer latency in Trp53 heterozygous mice. *Radiat Res* 2017;188:505–11.
31. Lemon JA, Phan N, Boreham DR. Multiple CT scans extend lifespan by delaying cancer progression in cancer-prone mice. *Radiat Res* 2017;188:495–504.
32. Shibamoto Y, Kamei Y, Kamei K *et al.* Continuous low-dose-rate irradiation promotes growth of silkworms. *Dose Response* 2017;15. https://doi.org/10.1177/1559325817735252.
33. Nakashima M, Sugie C, Wang Z *et al.* Biological effects of continuous low-dose-rate irradiation in silkworms and mice: growth promotion and tumor transplantability. *Dose Response* 2018;16. https://doi.org/10.1177/1559325818811753.
34. Löbrich M, Rief N, Kühne M *et al.* In vivo formation and repair of DNA double-strand breaks after computed tomography examinations. *Proc Natl Acad Sci U S A* 2005;102:8984–9.
35. Beucher A, Birraux J, Tchouandong L *et al.* ATM and Artemis promote homologous recombination of radiation-induced DNA double-strand breaks in G2. *EMBO J* 2009;28:3413–27.
36. Rothkamm K, Kühne M, Jeggo PA *et al.* Radiation-induced genomic rearrangements formed by nonhomologous end-joining of DNA double-strand breaks. *Cancer Res* 2001;61:3886–93.
37. Banáth JP, MacPhail SH, Olive PL. Radiation sensitivity, H2AX phosphorylation, and kinetics of repair of DNA strand breaks in irradiated cervical cancer cell lines. *Cancer Res* 2004;64:7144–9.
38. Macphail SH, Banáth JP, Yu TY *et al.* Expression of phosphorylated histone H2AX in cultured cell lines following exposure to X-rays. *Int J Radiat Biol* 2003;79:351–9.
39. Yoshikawa T, Kashino G, Ono K *et al.* Phosphorylated H2AX foci in tumor cells have no correlation with their radiation sensitivities. *J Radiat Res* 2009;50:151–60.
40. Ichijima Y, Sakasai R, Okita N *et al.* Phosphorylation of histone H2AX at M phase in human cells without DNA damage response. *Biochem Biophys Res Commun* 2005;336:807–12.
41. Venkateswarlu R, Tamizh SG, Bhavani M *et al.* Mean frequency and relative fluorescence intensity measurement of γ-H2AX foci dose response in PBL exposed to γ-irradiation: an inter- and intra-laboratory comparison and its relevance for radiation triage. *Cytom Part A* 2015;87:1138–46.
42. Roch-Lefévre S, Mandina T, Voisin P *et al.* Quantification of γ-H2AX foci in human lymphocytes: a method for biological dosimetry after ionizing radiation exposure. *Radiat Res* 2010;174:185–94.
43. Ruiz de Almodóvar JM, Núñez MI, McMillan TJ *et al.* Initial radiation-induced DNA damage in human tumour cell lines: a correlation with intrinsic cellular radiosensitivity. *Br J Cancer* 1994;69:457–62.
44. Whitaker SJ, Ung YC, McMillan TJ. DNA double-strand break induction and rejoining as determinants of human tumour cell radiosensitivity. A pulsed-field gel electrophoresis study. *Int J Radiat Biol* 1995;67:7–18.

45. Deckbar D, Jeggo PA, Löbrich M. Understanding the limitations of radiation-induced cell cycle checkpoints. *Crit Rev Biochem Mol Biol* 2011;46:271–83.
46. Forand A, Dutrillaux B, Bernardino-Sgherri J. γ-H2AX expression pattern in non-irradiated neonatal mouse germ cells and after low-dose γ-radiation: relationships between chromatid breaks and DNA double-strand breaks. *Biol Reprod* 2004;71:643–9.
47. Af Hällström TM, Zhao H, Tian J *et al.* A tissue graft model of DNA damage response in the normal and malignant human prostate. *J Urol* 2014;191:842–9.